Vector Control of a Synchronous Reluctance Motor Including Saturation and Iron Loss

Longya Xu, Xingyi Xu, *Member, IEEE,* Thomas A. Lipo, *Fellow, IEEE,* and Donald W. Novotny, *Fellow, IEEE*

Abstract—**The application of vector control to a conventional synchronous reluctance motor (VCSynRM) is presented with emphasis on the effects of saturation and iron losses. It is shown experimentally that these parasitic effects can significantly influence the performance of a VCSynRM. A simplified steady-state *d-q* model including saturation and iron losses is presented, and experimental results concerning optimal torque/ampere and optimal efficiency operation are shown to be in general agreement with the predictions of the model.**

Introduction

HISTORICALLY, the performance of the line-start synchronous reluctance machine (SynRM) was regarded as inferior to that of the other types of ac machines, and thus, little attention has been directed to it recently. In recent years, although tremendous progress has been made in the variable-reluctance motor (VRM) [1], [2] and the unique attributes of the reluctance machine, such as simple and rugged structure and very good compatibility with the power electronic converter, have been recognized, the application of the more conventional SynRM in converter-fed variable-speed drives has not been examined in detail.

There are a number of advantages associated with a converter-fed SynRM [3]–[5]:

1) No starting cage is necessary. The rotor can therefore be designed purely for synchronous performance.
2) Electronic control makes the motor autosynchronous and can ensure an optimum torque angle at all loads and speeds. This permits the motor to operate without concern for pullout.
3) No damper winding is required to stabilize operation. This makes it possible to design the rotor for the highest possible reactance difference $X_d - X_q$, thus increasing the power density of the motor [2].

It is therefore important that research be conducted regarding the potential of the reluctance motor. In particular, vector control of the conventional synchronous reluctance machine, which is parallel to the field-orientation control of the synchronous or induction machine, deserves a special effort so that the capability of a SynRM can be fully utilized.

Issues such as efficiency and torque/ampere are important in evaluating the performance of an electric machine. Such characteristics depend on the losses and saturation behavior of the machine and therefore require experimental evaluation. However, a model is very useful in understanding the way in which various losses and nonlinearities impact performance. To assist in this regard, a synchronous reference frame steady state model of a SynRM including saturation and iron losses is developed. The behavior of a vector-controlled SynRM is analyzed based on the model. It is observed that saturation and iron losses can have a significant effect on the performance of a VCSynRM. To verify the validity of the model for vector control, a digital signal processor (DSP) based vector controller was built for a 7.5-hp SynRM to experimentally evaluate performance.

Equivalent Circuit of Synchronous Reluctance Motor

As illustrated in Fig. 1(a), a synchronous machine is typically equipped with three phase, symmetrical, sinusoidally distributed windings. Conceptually, a resistor R_m coupled to the total stator flux is added to incorporate iron losses. This resistor can be used to account for the main flux core losses in the stator iron. High-frequency core losses caused by flux pulsations in the rotor core are not correctly represented by R_m and are neglected in this paper. For the purpose of analysis, the equations of the sinusoidally operated reluctance machine can be conveniently expressed in the rotor reference frame by the well known *d-q* transformation [10]. These equations are summarized in Appendix A, and the resulting steady-state *d-q* equivalent circuits are shown in Fig. 1(b). Parameter identification will be discussed in the section on experimental results.

The treatment of saturation has been considered in detail by a number of authors [6]–[9], and numerous methods with varying levels of complexity are available. In this paper, the first-order approximation of simply representing the relation between λ_{ds} and i_{dm} by a saturation curve is employed. It is assumed, and confirmed by the experimental results, that the q axis does not saturate significantly and that there is negligible cross coupling between the d and q axes caused by saturation.

Note the difference between the current pair (i_{qm}, i_{dm}) compared with (i_{qs}, i_{ds}). If the iron loss is neglected, i.e.,

Paper IPCSD 91-18, approved by the Industrial Drives Committee of the IEEE Industry Applications Society for presentation at the 1990 Industry Application Society Annual Meeting, Seattle, WA, October 7–12. Manuscript released for publication February 12, 1991.

L. Xu is with the Department of Electrical Engineering, Ohio State University, Columbus, OH 43210-1272.

X. Xu is with Square D Company, Palatine, IL 60067.

T. A. Lipo and D. W. Novotny are with the Department of Electrical and Computer Engineering, University of Wisconsin, Madison, WI 53706-1691.

IEEE Log Number 9100944.

0093-9994/91/0900-0977$01.00

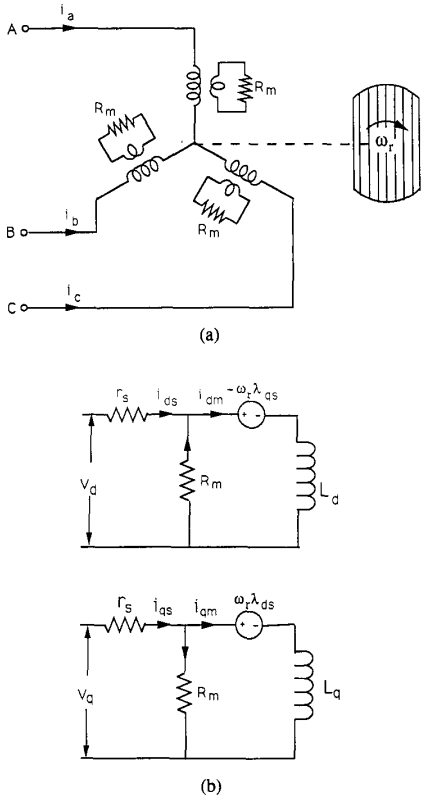

Fig. 1. Structure and equivalent circuit of a SynRM: (a) Structure of a SynRM; (b) equivalent circuit in rotor reference frame.

R_m approaches infinity, these two current pairs become equal. In this case, the stator MMF is aligned with the stator current. When R_m is finite, however, a phase difference between the stator current and MMF occurs due to the current in R_m. The relation between vectors I_{dqs}, I_{dqm}, and λ_{dqs} is shown in Fig. 2.

The electromagnetic torque produced can be obtained based on energy balance and the induced speed voltage as

$$T_e = \tfrac{3}{2}\left(\lambda_{ds} i_{qm} - \lambda_{qs} i_{dm}\right). \tag{1}$$

The torque is interpreted as the interaction between the flux linkage λ_{dqs} and the current I_{dqm}, and it is assumed that the effect of the flux nonlineraty can be taken into account by means of the saturation curve relating λ_{ds} and the current I_{dm}. The torque equation and the circuits of Fig. 1(b) form a useful conceptual and first-order analytical model to assist in understanding saturation and core loss impacts on SynRM performance.

Vector Control of a SynRM Without Saturation and Iron Losses

When saturation and iron losses are neglected, R_m approaches infinity. The d-q quantities are decoupled in this case, and vector control of the machine becomes trivial.

It is often desirable to achieve optimal efficiency operation of a SynRM. This can be achieved by selecting an appropriate current angle θ with respect to the rotor d axis. It can be easily shown that the optimal angle is 45° when only the winding I^2R is considered, and the saturation and iron losses are neglected. This is also the angle for maximum torque/ampere operation [4].

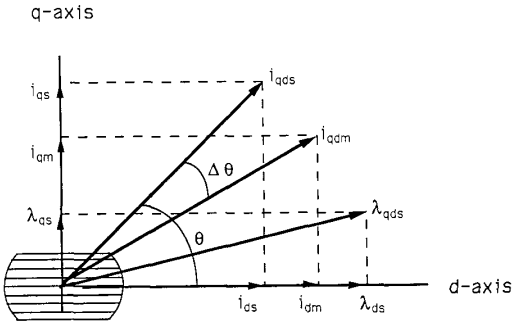

Fig. 2. Vector diagram of a SynRM for finite R_m.

Effects on Vector Control Caused by Saturation and Iron Loss

An approach to including the saturation effect of the iron is to assume that the torque equation remains true except that inductances in the d and q axes are excitation-current dependant. Note in particular that the saturation effect in the d axis is expected to be very different from that of the q axis because the nature of the magnetic paths are different. In the d axis, the magnetic path is iron dominant and excitation sensitive, whereas in the q axis, the magnetic path is air dominant and not excitation sensitive. Hence, an unequal saturation effect occurs on the d and the q axes, respectively, as the current increases. Under such a circumstance, to properly control the angle θ to optimally allocate the components i_{ds}, i_{qs} becomes complex.

While saturation alone increases the complexity of vector control, the iron loss will further complicate the situation. As illustrated by the d-q transformation, to represent the effect of the iron loss, an additional resistor R_m needs to be added to the equivalent circuit. It is of importance to realize that in the vector-controlled reluctance motor, the shunting resistor will share the input stator current. Hence, the physical stator currents are no longer the currents that directly govern the electromagnetic torque. In effect, a new magnetizing current I_{qdm} is defined by the component currents I_{qm} and I_{dm}, as is shown in Fig. 2. Comparing vectors I_{qds} and I_{qdm} shows that an additional angle shift $\Delta\theta$ is generated due to the iron loss. In effect, R_m adds an additional coupling mechanism to the d and q circuits, which can aggravate the misplaced stator current vector. It is evident that controling the current components i_{dm}, i_{qm} via vector control of the stator MMF for optimal torque/amp or optimal efficiency operation becomes more complex.

Configuration of Experimental System

Vector control of the experimental synchronous reluctance machine is implemented on a DSP-based system. Fig. 3 shows a diagram of the system. The experimental machine

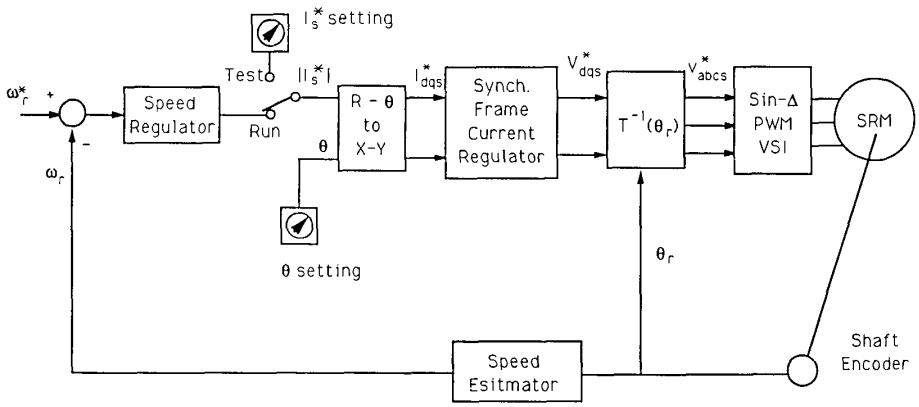

Fig. 3. Block diagram of the experimental system.

has an axially laminated rotor and a conventional three-phase stator winding. Appendix B describes the experimental machine and the induction machine from which the experimental machine was derived. The core losses of the machine are relatively large, which serves to enhance the evaluation of their impact on VCSynRM performance and on the validity of the dq circuit model.

Experimental Results

A. Parameter Identification

In order to identify L_q, R_m and the saturation curve, we need to align the actual stator flux to the d and q axes of the rotor, respectively. The alignment of stator flux with one of the axes can be determined by detecting zero shaft torque. In the experiment, the selecting switch in the block diagram is switched to the position of "test." Hence, the speed loop is opened, and the magnitude of the stator current I_s becomes an independent input variable. The speed is held constant by a dc dynamometer (800 r/min). For a given I_s input, the angle θ is adjusted around 0° (for d-axis alignment) or 90° (for q-axis alignment) until zero torque is reached. Phase current, fundamental input voltage, and input power are then measured. The parameters are calculated from the measured quantities.

The saturation curve (λ_{ds} versus i_{dm}) and iron loss resistor R_m are identified with the flux aligned with the d axis. In this case, the following equations can be derived from the equivalent circuit (neglecting the stator resistance):

$$V_s \approx V_{qs} \approx \omega_e \lambda_{ds} \tag{2}$$

$$I_{dm} = I_{ds} = I_s \cos(\theta) \tag{3}$$

$$P_{\text{iron}} = P_{in} - \tfrac{3}{2} I_s^2 R_s \tag{4}$$

$$R_m = \frac{3(\omega_e \lambda_{ds})^2}{2P_{\text{iron}}}. \tag{5}$$

The measured results are summarized in Table I.

Note that R_m is not constant but varies with λ_{ds}. This result occurs because the actual iron loss varies less rapidly than λ_{ds}^2 because of the hysteresis loss. If the actual iron loss varied as λ_{ds}^2, R_m would be a constant.

TABLE I
d-Axis Alignment Test for ω_r = 800r/min (ω_e = 26.67 rad/s)

θ^0	I_{spk}	Fund. V_s	P_{in}	I_{dm}	λ_{ds}	R_m
26.15	3.15	18.62	45	2.831	0.1111	12.65
20.52	8.27	52.17	267	7.75	0.3114	17.02
18.49	12.84	75.07	504	12.18	0.4480	19.27
13.65	21.37	91.28	775	20.77	0.5447	21.04
12.24	25.31	93.90	862	24.74	0.5603	21.74
11.36	28.61	97.00	950	28.05	0.5788	22.55

Information concerning L_q can be obtained by aligning the flux to the q axis. In this case, the stator resistance can no longer be neglected since the voltage is comparable to the IR drop. Recognizing that $\theta \approx 90°$ and $I_s \approx I_{qs}$, an approximation of L_q can still be derived from the equivalent circuit:

$$L_q^2 \approx \frac{V_s^2 - R_s^2 I_s^2}{\omega_e^2 I_s^2}. \tag{6}$$

This equation suggests that measurement of L_q is sensitive to the error in R_s. To minimize the sensitivity, the test should be conducted at a higher speed. At 800 r/min, L_q is estimated to be 0.0055 H for the tested machine. The unsaturable value of the L_q has also been verified by the finite element analysis for the current range from 0 to 20 A, and the calculated value is 0.0052 H.

B. Comparison Between Measured Performance and Model Prediction

With the parameters identified as above, we can use the equivalent circuit model to predict the performance of a SynRM. For simplicity, a fixed value of 18 Ω is used for R_m in the model, despite the variation in the actual R_m. The prediction is made for constant output speed (800 r/min) and constant output torque. The current angle θ is varied, and the corresponding stator current, input voltage, and input power are calculated.

An experiment was conducted to confirm the calculated performance. In this experiment, the speed loop is closed to maintain constant output speed. The load torque is maintained constant with a dc generator with a fixed load resistor

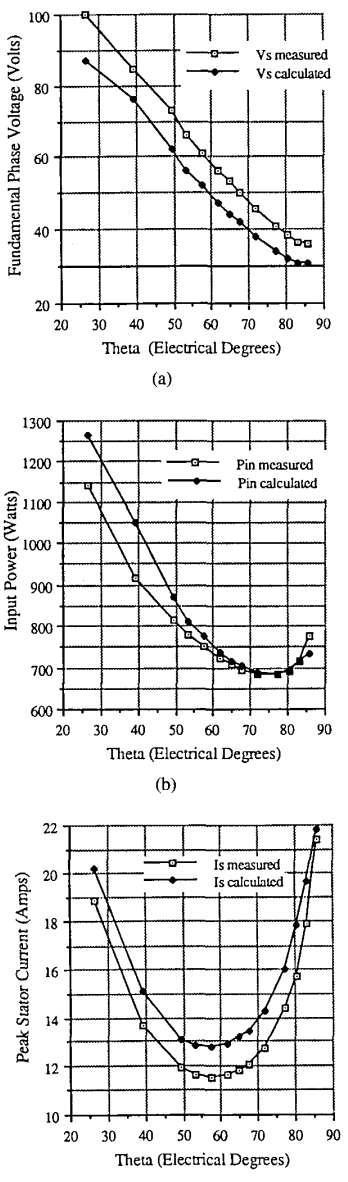

Fig. 4. Performance of VCSynRM (ω_{rm} = 800 r/min, T_e = 6.07 Nm): (a) Fundamental phase voltage; (b) input power; (c) peak stator current.

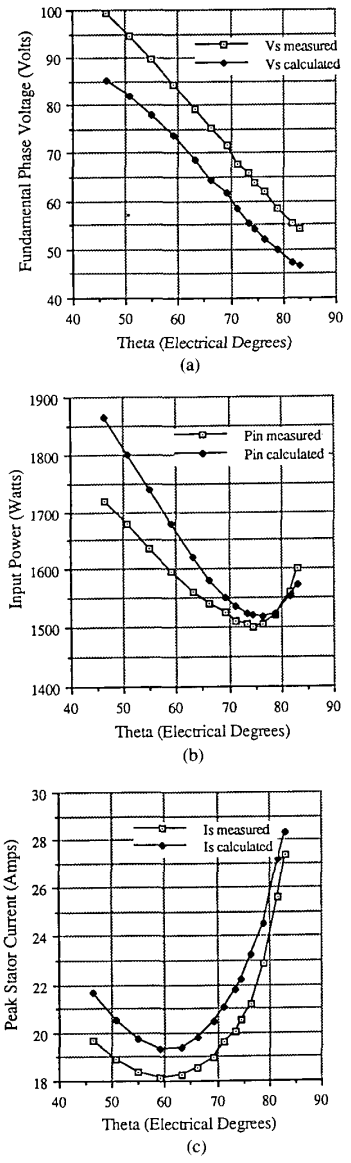

Fig. 5. Performance of VCSynRM (ω_{rm} = 800 r/min, T_e = 13.5 Nm): (a) Fundamental phase voltage; (b) input power; (c) peak stator current.

and fixed field excitation. The magnitude of stator current now becomes a dependent variable. Current angle is adjusted and corresponding stator current, input fundamental voltage, and input power are measured. The measured and calculated performance are compared in Figs. 4 and 5.

It is important to observe that the rotor angle for maximum torque per ampere and maximum efficiency is significantly different than the idealized value of 45° for both levels of loading. Note also that the predicted values of these optimal angles are in very good agreement with the measured values and that there is reasonable overall agreement between predicted and measured performance.

The reasons the actual angle differs from the idealized 45° for optimal torque/ampere can be understood as follows. It can be recalled from Fig. 2 that torque is generated when the flux λ_{qds} interacts with the current i_{qdm}. However, the flux λ_{ds} does not increase linearly with i_{dm}, which is the magnetizing current component. The best choice of the magnitude of the magnetizing current is such that the iron of the machine does not saturate significantly. This implies that the angle of the current needs to be controlled to ensure that the iron is at such a flux level. This requires an increased value of θ, which also increases i_{qm}, which is the armature current component in the q axis, and favors torque production for a given terminal current excitation.

The iron losses require an additional angle advance to

ensure optimal torque/ampere operation. This is clearly shown in the vector diagram in Fig. 2. Because of the iron losses, the effective current vector i_{qdm} is pushed back towards the d axis by an angle $\Delta\theta$. In order to have optimal torque/ampere operation, the physical current i_{qds} needs to be adjusted to an angle that is even larger than the angle needed when saturation is considered alone. To have optimal efficiency operation, an even larger increase in the current angle θ is required to further reduce the flux and hence the core loss. The optimum occurs when the additional I^2R loss associated with the increased q-axis current required to produce the torque offsets the reduction in core loss.

C. Effect of the Operating Frequency on the Optimal Current Angle

The equivalent circuit of the SynRM indicates that the iron loss is dependent on the operating frequency due to the speed voltage $\omega\lambda_{qdm}$. If the operating frequency is higher, the current through R_m will be larger, and hence, the iron loss is larger. Therefore, to implement vector control for the purpose of optimal efficiency or torque/ampere operation of the SynRM, the effect of frequency needs to be considered.

The machine model was utilized to calculate the current angle θ needed for optimal efficiency and torque/ampere operation with variable speed. The results are shown in Figs. 6 and 7.

As indicated in Fig. 6(a) and (b), the angle variation for optimal torque/ampere operation for different rotor speeds (frequencies) is small. This small angle change can be understood by inspecting the derived equivalent circuit and equations for parameter estimation. The calculated results have been compared with those obtained from experimental tests and shown in the same figure. The calculated results are, in general, correlated well with the experimental values.

On the other hand, as illustrated in Fig. 7, the current vector for optimal control of efficiency varies about 10 electrical degrees for rotor speed ranging from 400 to 1000 r/min. This significant change of the angle of the stator current vector results from the iron loss of the machine. In order to have a minimum input power for a given output power, the iron and copper loss should be optimally allocated, or equivalently, the magnetizing and armature current components must be properly controlled. Since the iron loss is nearly proportional to the square of the operating frequency, a large reduction of the flux linkage is required at high rotor speed to reduce the iron loss to an appropriate value. As shown in Fig. 7, when the machine is under light load, the current angle shift is still large because the magnetizing current component is dominant under this condition.

D. Transient Torque Control of the VCSynRM

Transient response to a torque command is always an important performance aspect to be considered for a converter-fed variable-speed drive. It is clear that in the VCSynRM, the magnitude and polarity of the torque can be changed rapidly by just shifting the current vector to a proper position with respect to the rotor saliency. For example, if the machine is initially rotating in the forward direction, by shifting the stator current vector to a negative angle with respect to the rotor d axis, the electromagnetic torque changes polarity, and the rotor will be braked to zero speed and then accelerated in reverse direction.

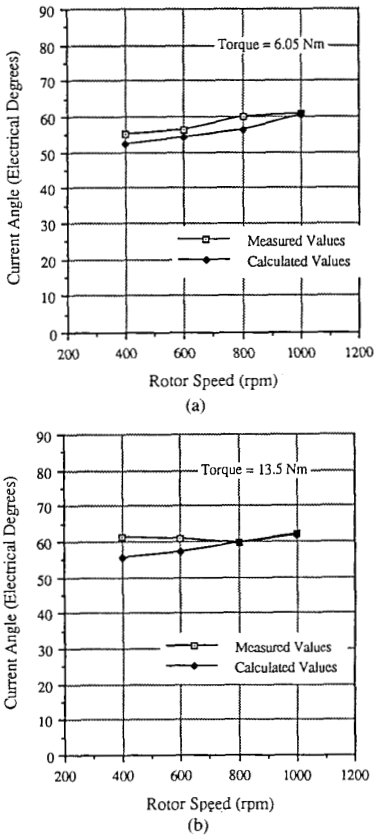

Fig. 6. Current vector angle for maximum torque/ampere: (a) 6.05 and (b) 13.5 Nm.

A control algorithm was implemented in the experimental drive system to ensure that for a given current, a maximum torque is produced. To implement the control algorithm, the optimal torque/ampere angle is calculated by the machine model and stored in a look-up table in the DSP. During VCSynRM operation, the microprocessor keeps accessing the table so that the current angle is always such that torque/ampere is maximized.

The transient response of the VCSynRM for both positive and negative step torque commands is shown by the rotor speed curve in Fig. 8. As shown in the figure, the SynRM is accelerated and decelerated alternatively with a controlled stator current vector. Note that this current vector has a constant magnitude but a positive angle in one direction and negative angle in the other direction. Therefore, the torque is expected to change polarity repetitively. Under such a circumstance, the machine experiences four quadrant operation, that is, two quadrant operation is in the motoring mode while another two are in the regenerative mode. The recorded rotor speed traces show that the system responds very quickly to the command, indicating that the step torque command is

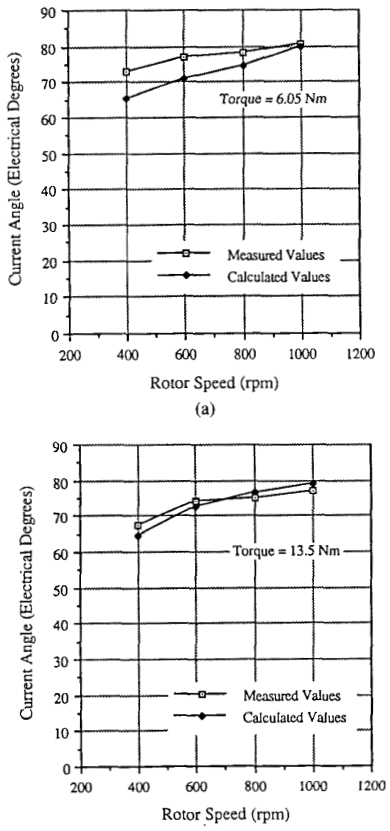

Fig. 7. Current vector angle for minimum P_{in}/P_{out}: (a) 6.05 and (b) 13.5 Nm.

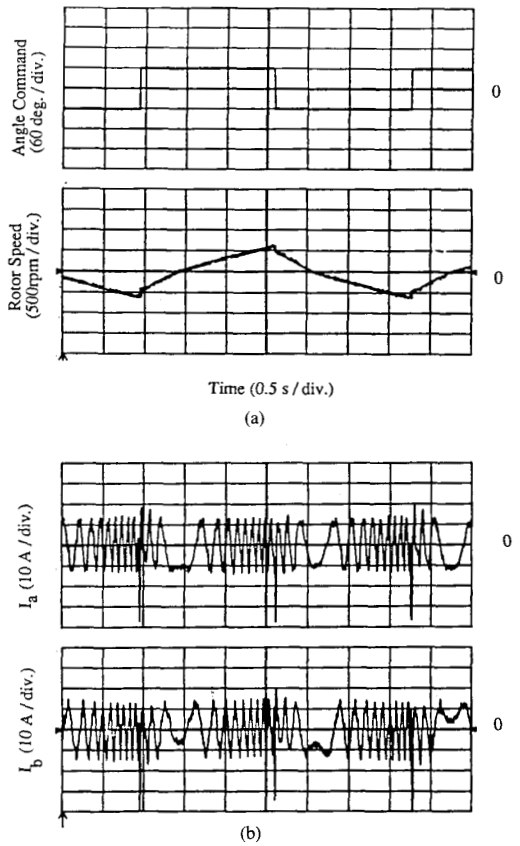

Fig. 8. Experimental results showing transient torque response: (a) Angle command and speed response; (b) phase current during torque transient.

followed properly. However, it has been observed from the experiment that the torque is not totally symmetric when the VCSynRM is operated in the motoring mode compared with the case where it is in the generating mode, that is, with the same value of stator current, the machine operating as a motor (positive current angle θ_0) a different value of torque is produced from the machine operating as a generator (negative current angle $-\theta_0$). The unsymmetrical torque response is clearly shown by the different speed slope of the machine when it is in the generator and motor mode, respectively.

The unsymmetrical torque response can be well explained by the *d-q* model of the SynRM shown in Fig. 2. Note, in particular, that when the defined terminal current vector reverses the angle while keeping the magnitude unchanged, the current source that supplies the circuit in the d axis will be unchanged, and the one powering the circuit in the q axis will have its direction reversed. With the defined terminal current, it can be shown that the resulting currents I_{qm} and I_{dm}, which directly govern the torque production, will make the torque value larger when the machine acts as a generator. This is actually a dual characteristic of a voltage-excited machine with a finite armature resistance.

To illustrate the discussion above, a vector diagram is drawn in Fig. 9. In this diagram, the imposed current vectors to the machine have the same magnitude but opposite angle.

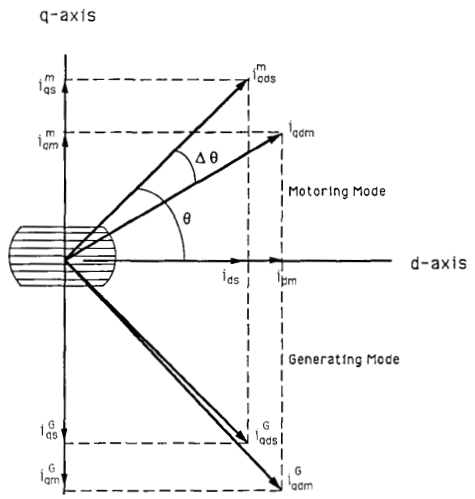

Fig. 9. Phasor diagram illustrating current vector in motoring and generating modes.

Note that due to the iron loss current through equivalent resistor R_m, in the generator case, the effective current vector i_{qdm} will change, in both magnitude and angle, to a point that favors the torque production. A control algorithm and implementation that compensate this unsymmetrical ef-

fect is being developed. It should also be mentioned that the unsymmetrical torque response in the motoring and regenerative mode caused by the iron loss is a common problem in other types of machine drives powered by a current source.

Conclusion

The results presented in this paper clearly show that saturation and iron loss can have a significant role in establishing optimal rotor angles for vector control of a SynRM. In general, the optimal angles for maximum torque/ampere and maximum efficiency are larger than the theoretical 45° angle predicted by a linear, lossless model. A simple first-order model incorporating the core losses as a shunt resistor and allowing saturation in the d axis yields useful insight into performance and provides a means for implementing control strategies to compensate for these effects.

APPENDIX A
d-q Transformation of the Phase Equations for the Sinusoidally Excited Reluctance Motor

1) Phase Description of the SynRM and Current Source: The machine discussed in the paper is assumed to have the structure shown in Fig. 1(a). Under this assumption, the self and mutual inductances of the machine can be described as a function of the rotor position and expressed by the matrix

$$[L_{abc}] = \begin{pmatrix} L_{aa} & L_{ab} & L_{ac} \\ L_{ba} & L_{bb} & L_{bc} \\ L_{ca} & L_{cb} & L_{cc} \end{pmatrix} \tag{A1}$$

with

$$\begin{aligned} L_{aa} &= L_0 - L_m \cos 2\theta_r \\ L_{bb} &= L_0 - L_m \cos 2(\theta_r - 2\pi/3) \\ L_{cc} &= L_0 - L_m \cos 2(\theta_r + 2\pi/3) \\ L_{ab} = L_{ba} &= -L_0/2 - L_m \cos 2(\theta_r - \pi/3) \\ L_{ac} = L_{ca} &= -L_0/2 - L_m \cos 2(\theta_r + \pi/3) \\ L_{bc} = L_{cb} &= -L_0/2 - L_m \cos 2(\theta_r + \pi). \end{aligned}$$

To include the effect of the stator iron loss, a resistor R_m is placed in parallel with the magnetizing inductance in each phase. Further, if the machine is powered by a three-phase balanced sinusoidal current source

$$[i_{abc}] = \begin{pmatrix} i_a \\ i_b \\ i_c \end{pmatrix} = \begin{pmatrix} I_m \cos\theta \\ I_m \cos(\theta - 2\pi/3) \\ I_m \cos(\theta + 2\pi/3) \end{pmatrix} \tag{A2}$$

then the armature resistance and stator winding leakage inductance can be excluded from the current equation. The phase current equation becomes, in matrix form

$$[i_{abc}] = [i^m_{abc}] + \frac{1}{R_m} p[\lambda^m_{abc}] \tag{A3}$$

where the current vector $[i^m_{qdn}]$ and flux linkage $[\lambda^m_{abc}]$ correspond to the quantities in Fig. 1.

2) d-q Transformation and Equivalent Circuit: Equation (A3) can be conveniently expressed in the rotor synchronous reference frame by the well-known d-q transformation [10]. The transformation is accomplished by multiplying both sides of (A3) with transformation matrix

$$T = \frac{2}{3} \begin{pmatrix} \cos\theta & \cos\left(\theta - \frac{2\pi}{3}\right) & \cos\left(\theta + \frac{2\pi}{3}\right) \\ \sin\theta & \sin\left(\theta - \frac{2\pi}{3}\right) & \sin\left(\theta + \frac{2\pi}{3}\right) \\ \frac{1}{\sqrt{2}} & \frac{1}{\sqrt{2}} & \frac{1}{\sqrt{2}} \end{pmatrix}. \tag{A4}$$

After the transformation, the matrix equation becomes

$$[i_{qdn}] = [i^m_{qdn}] + \frac{1}{R_m}\left\{\omega \times [\lambda^m_{qdn}] + \frac{d[\lambda^m_{qdn}]}{dt}\right\} \tag{A5}$$

where

$$\begin{aligned} [i_{qdn}] &= T[i_{abc}] \\ [i^m_{qdn}] &= T[i^m_{abc}] \end{aligned}$$

and

$$\frac{1}{R_m}\left\{\omega \times [\lambda^m_{qdn}] + \frac{d[\lambda^m_{qdn}]}{dt}\right\} = T\frac{1}{R_m} p[\lambda^m_{abc}]$$

or in scalar form

$$\begin{aligned} i_{qs} &= i_{qm} + \frac{1}{R_m}\left\{\omega\lambda^m_d + \frac{d\lambda^m_q}{dt}\right\} \\ i_{ds} &= i_{dm} + \frac{1}{R_m}\left\{-\omega\lambda^m_q + \frac{d\lambda^m_d}{dt}\right\}. \end{aligned}$$

The voltage equation of the circuit is

$$[v^m_{qdn}] = \omega \times [\lambda^m_{qdn}] + \frac{d[\lambda^m_{qdn}]}{dt}. \tag{A6}$$

For the machine described in Fig. 1, if the armature resistance and stator leakage is considered, the voltage equation is

$$[v_{abc}] = r_s[i_{abc}] + L_{ls} p[i_{abc}] + [v^m_{abc}] \tag{A7}$$

where the voltage vector $[v^m_{abc}]$ is the voltage across the magnetizing inductance, and L_{ls} is the inductance associated with the stator leakage flux linkage. Similarly, the voltage equation can be transformed into the d-q reference frame and becomes

$$[v_{qdn}] = r_s[i_{qdn}] + L_{ls} p[i_{qdn}] + [v^m_{qdn}]. \tag{A8}$$

The d-q equivalent circuit suggested by (A8) is shown in Fig. 1(b). If the rotor iron loss of the machine is considered, it can be shown that an additional resistance needs to be in parallel with the magnetizing inductance in the d-q equivalent circuit. A more detailed equivalent circuit of a SynRM, which includes stator and rotor iron losses, is shown in Fig. 10. Note that second-order effects such as rotor stray losses caused by harmonics due to slotting and flux distortion are

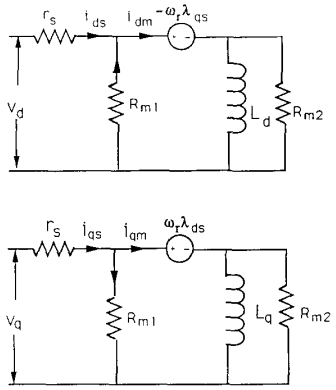

Fig. 10. Equivalent circuit of a SynRM including stator and rotor iron losses in synchronous d-q reference frame.

not considered by this model. One possible means to include the stray losses is to adapt the value of R_m based on experimental data since these losses are main flux dependent and the losses occur in the steady state.

APPENDIX B
Description and Specifications of the Experimental Synchronous Reluctance Motor

The experimental SynRM tested and discussed in this paper consists of a three-phase double layer wound stator and an axially laminated rotor. When the stator is excited with three-phase sinusoidal current, a rotating field will be created in the airgap. The stator is actually standard for a 7.5-hp three-phase induction machine.

The rotor is divided into four segments, and each segment is a stack of axially laminated common steel sheets sandwiched by nonmagnetic material. When the rotating field is aligned with the rotor laminations, the rotor provides maximum permeance, and thus, the airgap flux is maximized. Otherwise, when the rotating field is not aligned with the field, a large reluctance is encountered, which minimizes the airgap flux.

The specifications for the equivalent induction machine is listed in the following:

Ratings	
Power rating:	7.5 hp
Rated speed:	1750 r/min
Rated voltage:	230 V
Rated current:	10 A
Power factor at rated load:	0.8.
Geometry	
Stator lamination OD:	9.001 in
Stator lamination ID:	4.954 in
Effective length of stator stack:	4.00 in
Stator phase resistance:	0.2 Ω.

References

[1] P. J. Lawrenson, J. M. Stephen, P. T. Blenkinsop, J. Corda, and N. Fulton, "Variable-speed switched reluctance motors," *Proc. Inst. Elec. Eng.*, vol. 127, pt. B, no. 4, pp. 253-265, July 1980.

[2] L. Xu and T. A. Lipo, "Analysis of a variable speed singly-salient reluctance motor utilizing only two transistor switches," *IEEE Trans. Industry Applications*, vol. 26, no. 2, pp. 229-236, Mar./Apr. 1990.

[3] T. J. Miller, C. Cossar, and A. J. Hutton, "Design of a synchronous reluctance motor drive," in *Proc. IEEE IAS Ann. Mtg.*, Oct. 5, 1989, pp. 122-128.

[4] A. Chiba and T. Fukao, "A closed loop control of super high speed reluctance motor for quick torque response," in *Proc. IEEE IAS Ann. Mtg.*, 1987, vol. 1, pp. 289-294.

[5] A. Fratta and A. Vagati, "A reluctance motor drive for high dynamic performance applications," in *Proc. IEEE IAS Ann. Mtg.*, 1987, vol. 1, pp. 295-302.

[6] I. Boldea and S. A. Nasar, "Unified treatment of core losses and saturation in the orthogonal-axis model of electric machines," *Proc. Inst. Elec. Eng.*, vol. 134, pt. B, no. 6, pp. 355-363, Nov. 1987.

[7] E. Levi and V. Vuckovic, "Field oriented control of induction machines in the presence of magnetic saturation," *Elec. Machines Power Syst.*, vol. 16, no. 2, pp. 133-147, 1989.

[8] J. E. Brown, K. P. Kovacs, and P. Vas, "A method of including the effects of main flux path saturation in the generalized equations of ac machines," *IEEE Trans. Power App. Syst.*, vol. PAS-102, no. 1, pp. 96-103, Jan. 1983.

[9] K. P. Kovacs, "On the theory of cylindrical rotor ac machines including main flux saturation," *IEEE Power App. Syst.*, vol. PAS-104, no. 4, pp. 754-761, Apr. 1984.

[10] D. W. Novotny and R. D. Lorenz, "Introduction to field orientation and high performance ac drives," IEEE-IAS Tutorial Notes, in *Proc. IEEE-IAS Ann. Mtg.*, Oct. 1986.

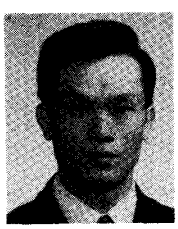

Longya Xu was born in Hunan, China. He graduated from Shangtan Institute of Electrical Engineering in 1970. He received the B.E.E. degree from Hunan University, China, in 1982 and the M.S. and Ph.D. degrees from the University of Wisconsin, Madison, in 1986 and 1990.

From 1971-1978, he participated in 150-kvA synchronous machine design, manufacturing, and testing in China. From 1982-1984, he worked as a researcher for linear electric machines in the Institute of Electrical Engineering, Sinica Academia of China. Since he came to the United States, he has served as a consultant to several industry companies including Raytheon Co., U.S. Wind Power Co., Pacific Scientific Co., and Unique Mobility Inc. for various industrial concerns. He joined the Department of Electrical Engineering at the Ohio State University in 1990, where he is presently an Assistant Professor. His research and teaching interests include power electronic control and converter optimized design of electrical machines and drive systems.

Dr. Xu received the 1990 First Prize Paper Award in the Industry Drive Committee.

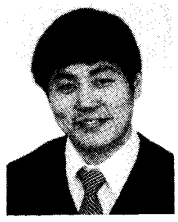

Xingyi Xu (M'90) was born in Nanchang, China. He received the B.S. degree in 1982 from Huazhong (Central China) University of Science and Technology, Wuhan, China. He received the M.S. and Ph.D. degrees in electrical engineering from the University of Wisconsin, Madison, in 1983 and 1990, respectively.

He has served as a consultant to several companies including Eaton Corporation, Kohler Company, and Baker Manufacturing on problems of electric machine design and power electronic control of drive systems. He is now with Square D Company. His research interests include modeling and simulation of electromagnetic devices and power electronic circuits, electric machines and drives, power quality problems, and microprocessor control systems.

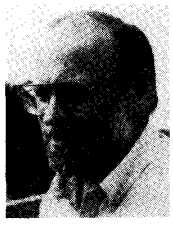

Thomas A. Lipo (M'64-SM'71-F'87) received the B.E.E. and M.S.E.E. degrees from Marquette University, Milwaukee, WI, in 1962 and 1964, respectively, and the Ph.D. degree in electrical engineering from the University of Wisconsin in 1968. He was an NRC Postdoctoral Fellow at the University of Manchester Institute of Science and Technology, Manchester, England, from 1968 to 1969.

From 1969 to 1979, he was an Electrical Engineer in the Power Electronics Laboratory of Corporate Research and Development of the General Electric Company, Schenectady, NY. He became Professor of Electrical Engineering at Purdue University, Lafayette, IN, in 1979 and later joined the University of Wisconsin, Madison, in the same capacity. He has been involved in the research of power electronics and ac drives for over 25 years.

Dr. Lipo has received 11 IEEE prize paper awards including corecipient of the Best Paper Award in TRANSACTIONS ON INDUSTRY APPLICATIONS for 1984. In 1986, he received the Outstanding Achievement Award from the IEEE Industry Applications Society for his contributions to the field of ac drives.

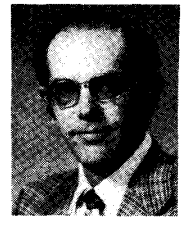

Donald W. Novotny (M'62-SM'77-F'87) received the B.S. and M.S. degrees in electrical engineering from the Illinois Institute of Technology, Chicago, in 1956 and 1957, respectively, and the Ph.D. degree from the University of Wisconsin, Madison, in 1961.

Since 1961, he has been a member of the faculty at the University of Wisconsin, Madison, where he is currently Professor and Co-Director of the Wisconsin Electric Machines and Power Electronics Consortium (WEMPEC). He served as Chairman of the Electrical and Computer Engineering Department from 1976 to 1980 and as an Associate Director of the University-Industry Research Program from 1972 to 1974 and from 1980 to the present. He has been active as a consultant to many organizations and a Visiting Professor at Montnana State University, Boseman, the Technical University of Eindhoven, Eindhoven, The Netherlands, the Catholic University of Leuven, Leuven, Belgium, and a Fullbright Lecturer at the University of Ghent, Ghent, Belgium. His teaching and research interests include electric machines, variable-frequency drive systems, and power electronic control of industrial systems.

Dr. Novotny is a member of ASEE, Sigma Xi, Eta Kappa Nu, and Tau Beta Pi, and is a Registered Professional Engineer in the State of Wisconsin.